Theor Chem Acc (1998) 99:143–150

Theoretical
Chemistry Accounts

Overview

Some fundamental questions in chemical reactivity

Juan Bertrán

Departament de Química, Universitat Autònoma de Barcelona, E-08193-Bellaterra, Barcelona, Spain

Received: 25 November 1997 / Accepted: 23 December 1997

Abstract. This paper provides an overview of recent progress on some fundamental questions in chemical reactivity. The following issues are emphasized: (1) the choice of electronic structure level for dynamics study; (2) Diels-Alder reactions; (3) combined molecular orbital/molecular mechanics methods; (4) solvent effects; (5) S_N2 reactions; (6) dynamics simulations; (7) proton-transfer reactions; and (8) femtochemistry.

Key words: Chemical reactivity – Diels-Alder reactions – S_N2 reactions – Proton-transfer reactions

1 Introduction

First of all I wish to emphasize the word "some" in the title. Of course, the selection is subjective, consequently, many questions and important contributions are going to be left out in this overview. I apologize in advance.

At present, one of the most interesting phenomena in the scenario of chemical reactivity is the "boom" of femtochemistry. By means of pump-probe delayed ultrafast laser pulses molecular dynamics may be followed in real time [1]. These experimental achievements have pushed theoretical studies to place greater emphasis on dynamics, which is the appropriate perspective in chemical reactivity. Nowadays, a large amount of classical, semiclassical and quantum dynamics studies are going on. Transition-state theory itself may be viewed as local dynamics at the dynamical bottleneck [2].

Although most femtochemistry studies deal with excited-state processes, ground-state processes have been studied as well. One of the most promising techniques is the direct observation of transition states in anion photodetachment spectra [3]. In this context it must be remarked that the definition of the transition state is broader than the usual one. It means the full family of configurations through which the reacting particles evolve en route from reagents to products [4, 5]. The variational theory of reaction rates further extends the range of transition state of interest and quantum considerations extend the range yet further. When one speaks about the direct observation of the transition state, the notion itself of transition state must be revisited. I shall mention, as an example, the transition-state spectroscopy of cyclooctatetraene [6]. The photoelectron spectrum of the planar cyclooctatetraene radical anion shows transitions to two electronic states. These states correspond to the D_{4h} $^1A_{1g}$ state, which is the transition state for ring inversion, and the D_{8h} $^3A_{2u}$. The transition state for bond shifting in cyclooctatetraene is planar with D_{8h} symmetry, but it is a singlet that it is not observed directly in the photoelectron spectrum. By the way, the D_{8h} $^1A_{1g}$ transition state of bond alternation lies well below the triplet, in a violation of Hund's rule.

The general problem, however, of direct inversion of the experimental spectra into a potential surface is intractable [7]. Consequently there is room for quantum chemistry in the study of chemical reactivity.

The first question is at what level ab initio calculations must be done in order to yield continuous potential energy surfaces with the same level of accuracy in the different regions. It is very well known that a single determinant wave function is not able to properly describe the dissociation of a molecule into atoms or fragments [8]. A similar difficulty is found in describing singlet diradical intermediates. One may question whether single reference methods, despite their success at equilibrium geometries, describe the transition-state region with the same accuracy. The reason is that in this region one deals with a general occurrence of near degeneracies of the electronic states. This is very clear in symmetry-forbidden reactions. In a hypothetical mechanism where the different planes of symmetry are conserved, the electronic-state diagram for the formation of cyclobutene from two ethylenes is presented in Fig. 1a. An avoiding crossing occurs in the transition state. At least, two configurations must be taken into account to describe properly the transition state. Of course this is a particular situation, but in some way may be generalized from the analysis of adiabatic surfaces into diabatic ones. The transition state appears as an avoiding crossing between two states with the electronic patterns of reagents and products (Fig. 1b). There is no unique

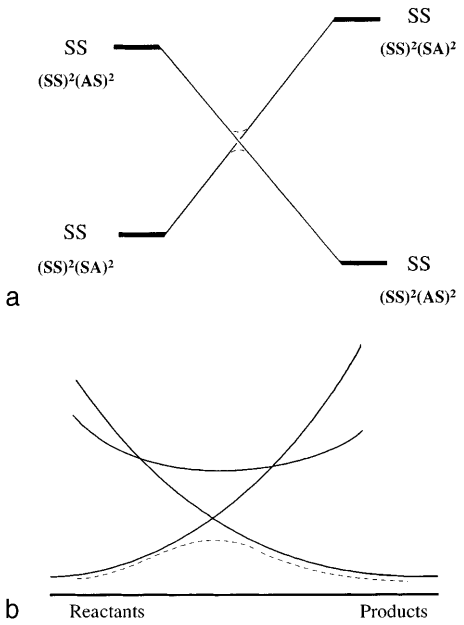

Fig. 1 **a** Electronic-state diagram for the formation of cyclobutene. **b** Adiabatic (.....) and diabatic (——) profiles for a general reaction

correspondence between valence-bond states and configurations in molecular orbital models. Nevertheless, the question of whether a monoreference wave function describes the transition states at the same level of accuracy as the reagents is open. The non-dynamical as well as dynamical electron correlation must be taken into account in order to get accurate values of the potential energy barrier. Furthermore, without introducing the correlation energy not only the potential barrier may not be accurately reproduced but the topology of the potential surface may be completely wrong.

A theoretical model, however, must adequately balance accuracy and feasibility. Siegbahn [9] distinguishes three periods in computational quantum chemistry. A semiempirical period starting in the 1950s, an ab initio one starting in the 1960s and the age of pragmatism starting in the 1980s. The G2 theory developed by Pople is a representative example of this new pragmatism [10, 11]. The computational power, however, is the practical bottleneck in the study of large chemical systems. For a long time, the MP2 method was the state-of-the-art for this kind of system, but nowadays density functional methods, in particular the hybrid B3LYP method [12–14], is taking over this role. The "boom" of density functional theory is probably the main phenomenon that is going on in computational chemistry. This became clear at the most recent meeting on quantum chemistry at Atlanta. As a matter of fact in two recent versions of modified G2, the MP2 method is replaced by B3LYP, in the geometry optimization and vibrational frequency calculations [15, 16].

The evolution of variational transition state theory has followed a similar process. In the interpolated variational transition state theory, high-level ab initio calculations are carried out at a few points along the reaction path and then all the reaction path information needed in the reaction rate calculation is interpolated based on the data at these points [17]. The next step is a dual-level direct dynamics method. Two levels of electronic structure are used: a "low-level" that is used at a large number of geometries along the MEP and a "high-level" which is required only at a few selected points. Instead of interpolating the reaction-path information directly, the corrections to the low-level values along the reaction path are interpolated based on the corrections at the selected points where high-level ab initio calculations have been carried out [18, 19]. Other improvements of the model are the use of curvilinear internal coordinates in vibrational frequencies [20] and the use of other more practical reaction coordinates than the MEP [21].

In the perspective of the pragmatic age with the main goal being to approach real systems, theoretical chemists have become aware that the environment must be taken into account in their studies on chemical reactivity. In the laboratory reactions take place normally in solution. Furthermore, frequently we are interested in enzymatic processes or heterogeneous catalysis. In this context where the solvent, the proteinic environment or the metallic surface must be considered, the "boom" of hybrid quantum mechanical and molecular mechanical (QM/MM) methods is the most interesting phenomenon. An excellent review of these methods may be found in Ref. [22]. In order to get free energy profiles by means of the free energy perturbation method, it must be stressed that the most critical point in many applications is not the accuracy of the potential energy function but the sampling issue [23]. This is especially true in the transition-state region when a geometric mapping method is used and solvent coordinates are an important part of the reaction coordinate itself. This problem arises from the fact that the geometric-mapping approach does not correctly sample the relevant solvent coordinates [24]. The solvent fluctuations defining the transition state will only be reached in a very long simulation.

At present, the question is not continuum vs. discrete models of the solvent. Continuum as well as QM/MM methods take into account the electronic and the nuclear relaxation of the solute in solution, although at a very different computational price. There is a complementarity between both methods. The real question is empirical vs. ab initio approaches. In continuum models as well as in standard Monte Carlo or molecular dynamics simulations empirical parameters are used. On the other hand, in ab initio molecular dynamics [25, 26] one uses interatomic forces computed directly from the electronic structure rather than requiring an empirical interaction potential as input. The choice of one or the other option is a question of mentality and the goal of the simulations.

Three typical reactions: Diels-Alder, S_N2 and proton-transfer processes have been chosen in order to illustrate the above mentioned questions.

2 Diels-Alder reaction

2.1 Mechanism

The concerted mechanism of the reaction is supported traditionally by the aromatic character of the transition

state. Recently, this point has been analysed from two different approaches. Herges and coworkers [27] apply magnetic properties as criteria to investigate the nature of the transition state, since aromatic compounds exhibit exalted diamagnetic susceptibilities. Although magnetic properties of the transition state cannot be measured experimentally, they can be computed conveniently. The magnetic susceptibility reaches its maximum in the region of the transition state for the Diels-Alder reaction. It indicates pronounced current effects, characteristic of cyclic electron delocalization and in consequence the Diels-Alder reaction may be catalysed by a magnetic field. In the second approach, within the valence-bond scheme, Bernardi and coworkers [28] have computed the delocalization energy in the transition states of allowed ($2\pi_s + 4\pi_s$) and forbidden ($2\pi_s + 2\pi_s$) cycloadditions. In their procedure a correlated complete-active-space self-consistent-field (CASSCF) wave function is rigorously transformed to a valence-bond space. The delocalization energies are −69.3 and −20.5 kcal/mol, respectively, leading to a smaller barrier for the Diels-Alder reaction than for the dimerization of ethylene. From the analysis of the different components, it is shown that 1,4 interactions, which can be related to Dewar structures, have an important stabilizing effect on the energy of the Diels-Alder transition state.

In spite of the favourable aromatic character in the concerted transition state, theorists have studied the mechanism of the parent Diels-Alder reaction at all feasible levels and have debated whether it has a concerted pericyclic or a stepwise mechanism, involving a diradical intermediate [29–32]. It is not easy at all to reproduce the potential energy barrier difference between both mechanisms, since both dynamical and non-dynamical correlation energy must be included in a balanced way, in order to obtain accurate relative energies of closed-shell and open-shell species.

In Table 1 the activation energy and the difference in activation energies of both mechanisms are presented at different levels of calculation using the 6-31G* basis set. CASSCF, which does not include dynamic electron correlation, yields a much higher barrier than QCISD(T), which does, and this illustrates the importance of including dynamic electron correlation for barrier heights. This aspect is more important in the concerted than in the diradical mechanism. In conclusion, CASSCF overestimates the stability of diradical species relative to closed-shell ones [33]. On the other hand, QCISD(T) seems not to describe correctly the non-dynamical electron correlation of diradical species. The B3LYP method supplies an activation energy comparable to QCISD(T)//CASSCF results and the best activation difference, especially after spin correction. The B3LYP method is capable of providing relatively economical direct comparisons of concerted and stepwise mechanisms. Furthermore, for the Diels-Alder reaction B3LYP works better than the MP2 method. At least the third-order (MP3) level is required to get acceptable activation energies.

Comparisons between theoretical and experimental secondary kinetic isotope effects [30–32, 34, 35] support a concerted and a synchronous mechanism for the parent reaction. Recently, the first femtosecond real-time study of the retro-Diels-Alder reaction of norbornene and norbornadiene, which are respectively products of the cycloaddition of cyclopendatiene with ethylene and acetylene, was carried out [36]. The results suggest that both channels are present. In both routes stereochemical retention is a consequence of the femtosecond C—C bond dynamical time scale. Unfortunately, there are no theoretical dynamic studies on the Diels-Alder reaction which allow one to interpret these femtosecond results.

2.2 Reactions with substituents

From a methodological point of view, an interesting recent development is transition-state modelling with empirical force fields [37, 38], where QM/MM calculations are combined. The simplest application of this methodology involves the use of a rigid transition state in the model system while the substituents are optimized at the MM level. A more sophisticated approach involves the use of a flexible transition-state model. In this case, the positions of all atoms are optimized. It requires the development of new MM parameters to describe the bond breaking/forming process.

Another original approach has been introduced by Froese et al. [39, 40] and Svensson et al. [41] for the study of Diels-Alder reactions with substituents. In the study of a large system, one faces the dilemma of studying the real system at a relatively low level of theory or studying a model system at a high level of accuracy. In the integrated MO + MO (IMOMO) model the total energy is approached by the expression [39, 40]:

$$E = E(\text{high,model}) + \{E(\text{low,real}) - E(\text{low,model})\}.$$

The model system is calculated at the G2 level, where corrections coming from high-level electron correlation and from large basis sets are included, while the difference in energy between the real and the model system is evaluated at a lower level. In a more sophisticated method, a multilayered integrated MO + MM method (ONIOM) [41], the active region, first layer, is

Table 1. Activation energy ($\Delta E^{\ddagger}$) and difference in activation energy ($\Delta\Delta E^{\ddagger}$) (in kcal/mol) between concerted and stepwise mechanisms in the Diels-Alder parent reaction, using the 6-31G* basis set

	Exp.	RHF	MP2	CASSCF	QCISD/T)// CASSCF	B3LYP
($\Delta E^{\ddagger}$)	27.5[a]	47.4[a]	20.0[a]	47.4[a]	29.1[a]	24.8[a]
($\Delta\Delta E^{\ddagger}$)	2–7[b]			1.9[b]	10[b]	8.8(3.4)[a]

[a] From Ref. [31]. Energies in *parentheses* are after spin correction.
[b] From Ref. [28.]

studied at a high level, the semi-active region, second layer, at a medium level and the non-active region, third layer, at a low level, frequently by means of MM. The small, the intermediate and the real systems are considered in a similar way to that in the previous method. By means of a code that combines the different gradients developed in a previous work [42], the stationary points of the real system are obtained. In particular, the IMOMO method allows inclusion of the effects of extended basis sets and higher-order electron correlation on bond energies by treating only a capped subsystem of a large molecule at a high level, and integrating this with a lower-level calculation on the entire system [43, 44].

The most frequent strategy, however, is to handle the whole system at the Hartree-Fock (HF), MP2 or B3LYP levels. The stereoselectivity, the regioselectivity and the diastereofacial selectivity are generally well reproduced in theoretical calculations at different levels. Nevertheless, to reproduce the endo-/exo-selectivity, at least HF/6-31G* calculations are required [45, 46]. The cause of the endo-selectivity is an open question. Frequently it has been explained by secondary interactions. For instance, in the addition of cyclopropene to butadiene, the endo-transition structure is stabilized due to the secondary interaction between a hydrogen atom of the cyclopropene and the π-bond of the butadiene [47, 48].

About the mechanism of unsymmetrical dienes or dienophiles, ab initio calculations predict normally concerted non-synchronous mechanisms. The degree of asymmetry increases with the nucleophilic or electrophilic character of the diene and the dienophile, respectively [49]. For the 1,1-diamino-butadiene to 1,1-dicyanoethylene reaction, a zwitterionic intermediate has been located when the solvent is included via the SCRF method [49]. On the other hand, a diradical mechanism has been proposed, using the B3LYP method, for the reaction between protoanemonics and butadiene which is in good agreement with experimental results [50].

Finally, I wish to present an example where the mechanism depends on the level of ab initio calculations. It is a Lewis-acid-catalysed Diels-Alder reaction. Given that the reaction is studied using a supermolecule approach, the same methodology as for the substituted reactions is used. The reaction between butadiene and acrolein BF_3 coordinated by acrolein leads to a $(2+4)$ process at the SCF level, but to a normal $(4+2)$ process at the MP2 one, using the same 6-31G* basis set in both calculations [51]. This example shows the necessity of including correlation energy not only to get accurate quantitative results but also to get correct qualitative conclusions. It is always dangerous to take geometries at a low level to carry out calculations at higher levels of theory. In Diels-Alder reactions, especially in the presence of heteroatoms, the inclusion of electron correlation significantly modifies the geometries of the stationary points obtained at the HF level [52].

2.3 Solvent effects

For a long time, Diels-Alder reactions were believed to be insensitive to the solvent, due to their apolar character. Nevertheless, in 1980 Rideout and Breslow found out that their rates can be dramatically accelerated in aqueous media [53]. Since then many studies have been devoted to this topic. An excellent review may be found in Ref. [54]. The reaction between cyclopentadiene and methyl acrylate has been studied using a classical continuum model [46]. The main result is that the geometry of the transition state and the reaction path itself are modified in solution. In particular, the asynchronicity of the reaction is enhanced by the solvent and the reaction coordinate becomes more asymmetric. One result of continuum models is that the endo-/exo-selectivity increases with the polar character of the solvent, generally due to the higher dipole moment of the endo-transition structure than the exo one [46, 54]. The polar character, however, of the transition-state structure is not the key to the Diels-Alder acceleration in aqueous solution. This is a big challenge for classical continuum models that mainly focus on the electrostatic term. This is why Cramer and Truhlar [55], Chambers et al. [56] and Giesen et al. [57] have developed a new continuum model, which takes into account explicitly hydrophobic as well as hydrophilic effects.

Recently Furlani and Gao [58] carried out Monte Carlo simulations to investigate the hydrophobic and hydrogen-bonding effects on Diels-Alder reactions. Although the solute geometries used are the ones determined in gas phase, the combined QM/MM potential used accounts for the effects of solute electronic polarization by the solvent. The results obtained for the reaction of cyclopentadiene with methyl vinyl ketone indicate that the hydrogen-bonding interaction and the hydrophobic effects contribute equally to transition-state stabilization. For the reaction of cyclopentadiene with isoprene the stabilization energy of the transition state is larger than in the previous case, and it is entirely attributed to the hydrophobic effect. Anyway, these findings indicate that hydrophobic effects play an important role in the rate enhancement of Diels-Alder reaction in aqueous solution.

3 S_N2 Reaction

3.1 Energy profiles

The S_N2 is another prototype organic reaction. Frequently a valence-bond approach has been used in its study. The transition state on the adiabatic surface arises from the avoiding crossing of two or more diabatic states. In this reaction, however, the coupling term between the diabatic states is large. Gas-phase identity and non-identity S_N2 reactions of halide anions and methyl halides have been studied at various levels of theory [59–62]. Despite the many theoretical and experimental studies that have been concluded to date, gas-phase barrier heights remain uncertain, and the values of these barriers have been the subject of continuing debate. It is accepted that the energy profile may be represented by a double-well potential curve, symmetric in identity and asymmetric in non-identity processes. Let us consider the chloride-exchange reaction as an exam-

Table 2. Complexation energies of the ion-molecule complex (ΔH_{comp}), overall barriers relative to reactants ($\Delta H^{\ddagger}_{ovr}$) and central barriers ($\Delta H^{\ddagger}_{cent}$) (in kJ/mol) for the reaction of Cl^- with CH_3Cl [57]

	ΔH_{comp}	$(\Delta H^{\ddagger}_{ovr})$	$(\Delta H^{\ddagger}_{cent})$
MP2/6-311+G(3*df*,2*p*)	43.8	20.7	64.6
G2+	44.0	11.5	55.5
B3LYP/6-311+G(3*df*,2*p*)	40.7	−4.5	36.2
Exp.	51.0 ± 8.4	4.2 ± 4.2	55.2 ± 8.4

ple. It appears in Table 2 that G2+ supplies the most reasonable values but, given the uncertainty of "experimental" results obtained by interpreting experiments by applying statistical theories, it is difficult to assure that non-dynamical electron correlation energy has been taken into account properly in this monoreference approach. The experimental data fall within the MP2 and B3LYP values, which appear to be the upper and lower bounds, respectively.

The possibility of nucleophilic substitution reactions with retention of configuration has been studied as well [63]. The minimum energy pathways for both back-side and front-side S_N2 reactions are found to involve the same ion-molecule complex as a starting point, with the front-side pathway becoming feasible at higher energies ($\Delta H^{\ddagger}_{cent} = 237.8$kJ/mol at the G2+ level). These results suggest that the chloride exchange in CH_3Cl, which has been found in gas-phase experiments at high energies, may be the first example of a front-side S_N2 reaction with retention of configuration at the saturated carbon. The effect of a counterion in both profiles has also been studied [64]. In the transition state with retention of configuration the coordination of the metal cation is on the same side of both entering and leaving halide ions and the central carbon is essentially a methyl cation. Therefore, the effect of the counterion is to decrease the potential barrier. In contrast, the barrier increases in the inversion process for two reasons. The first one is the strong distortion of the linear rearrangement of the transition structure, to allow the coordination of the metal cation with both halides. The second one arises from the fact that the metal cation interacts with a more delocalized negative charge at the transition state than in the reagents. As a consequence, both mechanisms become competitive.

Finally, let us present another example where the topology of the potential surface changes when the correlation energy is taken into account. The reaction $HS^- + HS\text{-}SH \rightarrow HS\text{-}SH + HS^-$ is an S_N2 reaction at the HF/6-31+G* level, while it is an addition-elimination process at the MP2/6-31+G* level [65, 66]. At the MP2 level the symmetric structure is an intermediate, while at the HF level it is a transition state.

3.2 Dynamics simulations

Dynamics simulations lead to a complex picture. Classical and quasiclassical trajectory simulations have been carried out on analytical potential surfaces derived from high-level ab initio calculations [67–69], and with semiempirical direct dynamics [70]. Non-statistical effects observed in classical trajectory simulations have been interpreted by means of a reaction path Hamiltonian analysis [71]. Finally, statistical rate theory calculations have supplied deep insight into these dynamical results [72–74]. An initial ion-molecule complex is formed with the energy non-statistically partitioned between the vibrational and relative translational modes of the two species. The crucial point is a weak coupling between the low-frequency intermolecular modes and the high-frequency intramolecular ones. As a consequence of this slow energy redistribution, many collisions rebound and the dissociation rate of the initial intermolecular complex is very high. On the other hand, for the same reason, the intramolecular complex may remain trapped in the vicinity of the central barrier and multiple crossing of this barrier may occur before the trajectory form the products or returns to the reagents. Due to this lack of statistical behaviour, the different statistical theoretical models are not able to explain the experimental results of the rate versus temperature, relative translational energy, methyl halide temperature and isotopic substitutions [72–74]. Recently, by means of a guided ion beam apparatus, the translational-energy threshold for the chlorine-exchange reaction has been found well above the previously reported potential energy barrier, due to non-statistical dynamical constraints [75].

Hu and Truhlar, however, using the canonical unified statistical theory, have obtained a reasonable agreement between theoretical previsions and experimental results for the kinetic isotope effects of the reaction between the chlorine anion and methylbromide [76]. On the other hand, Craig and Brauman found that the observed translational energy dependence is indistinguishable from that predicted by the Rice-Ramsperger-Kassel-Marcus theory for the reaction between the chlorine anion and chloroacetonitrile [77]. This suggests that the increased translational energy redistributes statistically in the collision complex. Therefore, non-statistical behaviour is not general to all gas-phase S_N2 reaction intermediates.

3.3 Solvent effects

The double-well energy profile of the chlorine-exchange reaction becomes unimodal in aqueous solution. In a way, it turns out to be easier to carry out molecular dynamics simulations in solution than in gas phase. As a matter of fact, most of the available solvent models have been used and tested to study static and dynamic effects of the solvent on this particular process, and have become prototype reactions for this purpose. The free-energy profiles in solution have been evaluated with both continuum and discrete solvent models. The solvent effect on the activation free energy is mainly electrostastic, and it is well reproduced in all the models. Two aspects, the transmission coefficient and the influence of solvent fluctuations on the process, have been specifically studied when considering the dynamic effects. The transmission coefficient at the top of the barrier has been

evaluated by means of stochastic treatments and molecular-dynamics simulations. The question of whether the reaction in solution is solvent-driven or solute-driven has merited less attention and remains an open question.

All this work was carried out at the end of the 1980s and at the beginning of the 1990s. Nowadays, this research continues to be active in three fields: the study of the reaction in supercritical water by means of molecular-dynamics simulations as well as continuum models [78–83]; the study of microsolvated clusters, to fulfill the gap between gas phase and solution [84–86] and finally, the use of continuum models for dealing with non-equilibrium or dynamic effects [87–91]. It seems more natural, however, to treat dynamical effects using molecular-dynamics simulations. This will be considered in the next section, where the coupling between the solvent fluctuations and the proton-transfer process will be analysed. At present this is a more lively topic.

4 Proton transfer reactions

4.1 Dynamics simulations

Proton-transfer processes as well as S_N2 reactions may be considered to be like inner-sphere-electron transfer processes. Several classical and quasiclassical trajectory simulations have been carried out on a variety of systems in gas phase. Using ab initio direct dynamics, selected reaction trajectories were calculated for the proton transfer between the hydronium ion and ammonium [92]. From ab initio fitted surfaces by means of quasiclassical trajectories the vibrational and rotational states of products in the proton-transfer reaction between the fluoride anion and hydrochloric acid have been discussed [93]. The dynamics of clusters $(H_2O)_nH^+$ ($n = 1,2,3,4$) interacting with an NH_3 molecule have been studied by first-principles Born-Oppenheimer molecular dynamics (BOMD) simulations [94]. The intramolecular proton transfer in the enol form of acetylacetone is calculated based on classical and Feynman path integral quantum transition-state theory, the transmission coefficient being obtained from activated dynamics for the classical system [95]. It is observed that there are significant differences between classical and QM calculations caused mainly by the lack of tunnelling effects in the former. The concerted proton transfer in cyclic water and hydrogen fluoride clusters [96], the intramolecular proton transfer in glycolate anion [97], the intermolecular hydrogen transfer between the trans-diazene and a hydrogen atom [19, 98] and C—H bond activation reactions [99] have been evaluated by means of the variational transition-state theory with interpolated corrections and dual-level direct dynamics, using various multidimensional semiclassical models of tunnelling.

In order to examine the role of the solvent fluctuations in the process, let us progress to studies of proton transfer in solution. First of all, classical dynamic studies will be mentioned. Quantum effects of the proton are minimized by using deuterium instead of hydrogen. By means of ab initio molecular-dynamics simulations Tuckerman et al. have studied the proton transport in water [100, 101]. Using the hybrid QM/MM method, where the chemical system is evaluated by density functional theory and the water molecules by MM with the TIP3P potential, the proton (deuterium) transfer in the $H_3O_2^-$ system has been studied [102]. The O—O distance was fixed at 2.9 Å and the proton was constrained to move along the line connecting the oxygen atoms. Given the low activation barrier many reactive events occur in the molecular-dynamics simulations. In order to analyse the coupling of proton transfer with solvent fluctuations, the solvent electric field along the O—O vector was calculated at the mid-point between the oxygens. The average value at the initial well is 0.02 a.u., and that at the transition state is 0.00 a.u.. The fluctuation of this electric field is ± 0.01 a.u. both when the position of the proton is constrained at the initial minimum and when it is constrained at the transition-state structure. The large magnitude of the electric field fluctuations predicted by these simulations can account for substantial modifications of the barrier. As a matter of fact there is a clear correlation between the plots of the proton position and the electric field as functions of the time elapsed in the simulation. The proton jump starts in a favourable value of the solvent fluctuation. The solvent electric field follows the proton jump with a small delay. After the transfer, the solvent starts to relax, and one notes that frequently it is not completely equilibrated by the time the next proton jump is produced. Many proton jumps take place when the solvent electric field is within the fluctuations of the transition state. The O—O constraint may be avoided in two different ways: by introducing an external harmonic field [103, 104] or by considering an intramolecular proton transfer. In this case, the same authors have found that the proton jump takes place when both the fluctuation of the solvent and that of the heavy atoms are favourable.

As it has been mentioned previously the proton is a light atom and must be handled with quantum dynamics. Many authors [26, 105–119] have presented mixed quantum-classical molecular dynamics (QCMD) methods, where the proton is treated by QM and the remaining nuclei are treated classically. The hydrogen atom moves on a potential dictated by the position of the classical particles, including of course solvent molecules, with a proper feedback of the quantum particles on the classical forces. Some authors [120–122] have emphasized that the solvent and the position of heavy atoms define the reaction coordinate, since they determine the energy profile for the delocalized description of the proton. The proton wave function is localized in the well of the reagents or of the products when the corresponding potential energy well is clearly deeper than the other. On the contrary, in the symmetric double well it is delocalized in both wells when the first vibrational level is over the potential barrier or when the spilitting of low vibrational levels is important, being the tunnelling dependent on the gap between the two adiabatic states.

In particular, Bala et al. have studied proton transfer in enzymes by means of a QCMD model [123]. Coupling between the quantum proton and the classical atoms is accomplished via extended Hellmann-Feynman forces.

A parametrized empirical valence bond potential surface fitted to reproduce ab initio results has been used. The first step of a hydrolytic process catalysed by phospholipase A_2 has been studied. The proton transfer between a water molecule and the imidazole of His47 may be followed through the mean proton position of a one-dimensional Gaussian wavepacket located initially in the global energy minimum. The most amazing result is that while in classical molecular dynamics the proton transfer does not occur, a proton jump is observed in QCMD simulations, showing the significant contribution of quantum effects. The jump of the proton occurs at a moment where the electrostatic field created by the proteinic environment is high in the hydrogen atoms of the water molecule. This suggests a mechanism similar to that observed in polar solvents, where proton-transfer processes occur towards prepared product states.

4.2 Femtochemistry

Intramolecular as well as intermolecular proton transfers have been studied by femtochemistry [1, 124]. In particular, proton transfers between an excited state of phenol and ammonium clusters of different size have been explored [125–127]. The pump-laser pulse prepares the wavepacket in the excited state, where the proton transfer takes place. The probe pulse, after different time delays, allows detection of the increase of products and the decrease of reagents by mass spectrometry due to multiphoton ionization. The occurrence of the proton transfers on the picosecond time scale was observed for ammonia clusters over four molecules. Furthermore, the decay is biexponential, the fast time response being ascribed to the proton transfer and the slow time response to solvent-cluster reorganization.

These fascinating experimental results have been interpreted by the hypothesis of a high potential barrier for the proton transfer in the ionized state. Nevertheless, theoretical calculations at different levels do not confirm this hypothesis at all [128, 129]. The proton transfer in the ionized state implies meaningful geometric changes not only in the region where proton transfer takes place but also in the aromatic ring that moves to a quinoidal structure after the process. It seems that the interpretation of the experimental results requires a theoretical dynamics study in order to follow the initial wavepacket formed by Franck-Condon pumping. It must be remarked that the potential surface of the ionized state has a high multidimensionality where intramolecular vibrational energy redistribution may play an important role. Carrying out this kind of dynamics study is one of the most important challenges for the future.

In this overview on chemical reactivity some achievements and challenges for the future have been presented. Femtochemistry has been introduced as the starting and finishing point of our journey because its impact is going to fix the future developments of chemical reactivity. At present the goal of femtochemistry is not only to follow molecular dynamics in real time but also to control the outcome of a chemical reaction [1, 130]. The control of chemical reactions is the main purpose of theoretical studies in chemical reactivity. Of course, the theoretical study of chemical reactivity is not an easy field at all, but it is a fascinating one.

References

1. Zewail AH (1996) J Phys Chem 100: 12701
2. Truhlar DG, Garrett BC, Klippenstein SJ (1996) J Phys Chem 100: 12771
3. Bradforth SE, Arnold DW, Newmark DM, Manolopoulos DE (1993) J Chem Phys 99: 6345
4. Polanyi JC, Zewail AH (1995) Acc Chem Res 28: 119
5. Topaler MS, Truhlar DG, Chang XY, Piecuch P, Polanyi JC (1998) J Chem Phys (in press)
6. Wenthold PG, Hrovat DA, Borden WT, Lineberger WC (1996) Science 272: 1456
7. Bacic Z, Miller RE (1996) J Phys Chem 100: 12945
8. Head-Gordon M (1996) J Phys Chem 100: 13213
9. Siegbahn EM, Blomberg MRA, Svensson M (1994) Chem Phys Lett 223: 35
10. Curtiss LA, Raghavachari K, Trucks GW, Pople JA (1991) J Chem Phys 94: 7221
11. Curtiss LA, Raghavachari K, Pople JA (1993) J Chem Phys 98: 1293
12. Becke AD (1993) J Chem Phys 98: 5648
13. Lee C, Yang W, Parr RG (1988) Phys Rev B 37: 785
14. Stevens PJ, Devlin FJ, Chablowski CF, Frisch MJ (1994) J Phys Chem 98: 11623
15. Bauschlicher CW, Partridge H (1995) J Chem Phys 103: 1788
16. Mebel AM, Morokuma K, Lin MC (1995) J Chem Phys 103: 7414
17. Gonzalez-Lafont A, Truong TN, Truhlar DG (1991) J Chem Phys 95: 8875
18. Hu WP, Liu YP, Truhlar DG (1994) J Chem Soc Faraday Trans 90: 1715
19. Chuang YY, Truhlar DG (1997) J Phys Chem 101: 3808
20. Jackels CF, Gu Z, Truhlar DG (1995) J Chem Phys 102: 3188
21. Villa J, Truhlar DG (1997) Theor Chem Acc 97: 313
22. Gao J (1995) In: Lipkowitz KB, Boyd DB (eds) Reviews in computational chemistry, vol 7. VCH, New York p 119
23. Kollman P (1993) Chem Rev 93: 2395
24. Muller RP, Warshel A (1995) J Phys Chem 99: 17516
25. Carr R, Parrinello M (1985) Phys Rev Lett 55: 2471
26. Tuckerman ME, Ungar PJ, Rosenvinge T, Klein ML (1996) J Phys Chem 100: 12878
27. Herges R, Jiao H, Schleyer PvR (1994) Angew Chem Int Ed Engl 33: 1376
28. Bernardi F, Celani P, Olivucci M, Robb MA, Suzzi-Valli G (1995) J Am Chem Soc 117: 10531
29. Li Y, Houk KN (1993) J Am Chem Soc 115: 7478
30. Storer JW, Raimondi L, Houk KN (1994) J Am Chem Soc 116: 9675
31. Houk KN, Gonzalez J, Li Y (1995) Acc Chem Res 28: 81
32. Goldstein E, Beno B, Houk KN (1996) J Am Chem Soc 118: 6036
33. Borden WT, Davidson ER (1996) Acc Chem Res 29: 67
34. Beno BR, Houk KN, Singleton DA (1996) J Am Chem Soc 118: 9984
35. Wiest O, Houk KN, Black KA, Thomas B (1995) J Am Chem Soc 117: 8594
36. Horn BA, Herek JL, Zewail AH (1996) J Am Chem Soc 118: 8755
37. Eksterowicz JE, Houk KN (1993) Chem Rev 93: 2439
38. Pascual-Teresa B, Gonzalez J, Asensio A, Houk KN (1995) J Am Chem Soc 117: 4347
39. Froese RDJ, Humbel S, Svensson M, Morokuma K (1997) J Phys Chem A 101: 277
40. Froese RDJ, Coxon JM, West SC, Morokuma K (1997) J Org Chem 62: 6991

41. Svensson M, Humbel S, Froese RDJ, Matsubara T, Sieber S, Morokuma K (1996) J Phys Chem 100: 19357
42. Maseras F, Morokuma K (1995) J Comput Chem 16: 1170
43. Coitino EL, Truhlar DG, Morokuma K (1996) Chem Phys Lett 259: 159
44. Coitino EL, Truhlar DG (1997) J Phys Chem 101: 4541
45. Jorgensen WL, Lim D, Blake JF (1993) J Am Chem Soc 115: 2936
46. Ruiz-Lopez MF, Assfeld X, Garcia JI, Mayoral JA, Salvatella L (1993) J Am Chem Soc 115: 8780
47. Sodupe M, Rios R, Branchadell V, Nicholas T, Oliva A, Dannenberg JJ (1997) J Am Chem Soc 119: 4232
48. Jursic BS (1997) J Org Chem 62: 3046
49. Sustmann R, Sicking W (1996) J Am Chem Soc 118: 12562
50. Branchadell V, Font J, Moglioni AG, Echaguen CO, Oliva A, Ortuno RM, Veciana J, Vidal-Gaucedo J (1997) J Am Chem Soc 119: 9992
51. Garcia JI, Mayoral JA, Salvatella L (1996) J Am Chem Soc 118: 11680
52. Barone V, Arnaud R (1997) J Chem Phys 106: 8727
53. Rideout DC, Breslow R (1980) J Am Chem Soc 102: 7816
54. Cativiela C, Garcia JI, Mayoral JA, Salvatella L (1996) Chem Soc Rev 1996: 209
55. Cramer CJ, Truhlar DG (1992) Science 256: 213
56. Chambers CC, Hawkins GD, Cramer CJ, Truhlar DG (1996) J Phys Chem 100: 16385
57. Giesen DJ, Hawkins GD, Liotard DA, Cramer CJ, Truhlar DG (1997) Theor Chem Acc 98: 85
58. Furlani TR, Gao J (1996) J Org Chem 61: 5492
59. Glukhovtsev MN, Pross A, Radom L (1995) J Am Chem Soc 117: 2024
60. Glukhovtsev MN, Pross A, Radom L (1996) J Am Chem Soc 118: 6273
61. Glukhovtsev MN, Bach RD, Pross A, Radom L (1996) Chem Phys Lett 206: 558
62. Deng L, Branchadell V, Ziegler T (1994) J Am Chem Soc 116: 10645
63. Glukhovtsev MN, Pross A, Schlegel HB, Bach RD, Radom L (1996) J Am Chem Soc 118: 11258
64. Harder S, Streitwiesser A, Petty JT, Schleyer PvR (1995) J Am Chem Soc 117: 3253
65. Bachrach SM, Mulhearn DC (1996) J Phys Chem 100: 3535
66. Mulhearn DC, Bachrach SM (1996) J Am Chem Soc 118: 9415
67. Hase WL, Cho YJ (1993) J Chem Phys 98: 8626
68. Hase WL (1994) Science 266: 998
69. Wang H, Peslherbe GH, Hase WL (1994) J Am Chem Soc 116: 9644
70. Peslherbe GH, Wang H, Hase WL (1996) J Am Chem Soc 118: 2257
71. Wang H, Hase WL (1996) Chem Phys 212: 247
72. Wang H, Hase WL (1995) J Am Chem Soc 117: 9347
73. Peslherbe GH, Wang H, Hase WL (1995) J Chem Phys 102: 5626
74. Wang H, Hase WL (1997) J Am Chem Soc 119: 3093
75. DeTuri VF, Hintz PA, Ervin KM (1997) J Phys Chem 101: 5969
76. Hu WP, Truhlar DG (1995) J Am Chem Soc 117: 10726
77. Craig SL, Brauman JI (1997) Science 276: 1536
78. Balbuena PB, Johnston KP, Rossky PJ (1994) J Am Chem Soc 116: 2689
79. Balbuena PB, Johnston KP, Rossky PJ (1995) J Phys Chem 99: 1544
80. Flanagin LW, Balbuena PB, Johnston KP, Rossky PJ (1995) J Phys Chem 99: 5196
81. Bennet GE, Rossky PJ, Johnston KP (1995) J Phys Chem 99: 16136
82. Pomelli CS, Tomasi J (1997) J Phys Chem 101: 3561
83. Tucker SC, Gibbons EM (1994) In: Cramer CJ, Truhlar DG (eds) Structure and reactivity in aqueous solution. Am Chem Soc Symp Ser 568: 196
84. Hu PW, Truhlar DG (1994) J Am Chem Soc 116: 7797
85. Oknno Y (1996) J Chem Phys 105: 5817
86. Re M, Laria D (1996) J Chem Phys 105: 4584
87. Mathis JR, Bianco R, Hynes JT (1994) J Mol Liq 61: 81
88. Aguilar M, Bianco R, Miertus S, Perico M, Tomasi J (1993) Chem Phys 174: 397
89. Basilevsky MV, Chudinov GE, Napolov DV (1993) J Phys Chem 97: 3270
90. Ruiz-Lopez M, Rinaldi D, Bertran J (1995) J Chem Phys 103: 9249
91. Truhlar DG, Schenter GK, Garrett BC (1993) J Chem Phys 98: 5756
92. Bueker HH, Helgaker T, Rund K, Uggerud E (1996) J Phys Chem 100: 15388
93. Tackikawa H (1995) J Phys Chem 99: 255
94. Cheng HP (1996) J Chem Phys 105: 6844
95. Hinsen K, Roux B (1997) J Chem Phys 106: 3567
96. Liedl KR, Sekusak S, Kroemer RT, Rode BM (1997) J Phys Chem 101: 4707
97. Fernandez-Ramos A, Rodriguez-Otero J, Rios MA (1997) J Chem Phys 107: 2407
98. Chuang YY, Truhlar DG (1997) J Chem Phys 107: 83
99. Espinosa-Garcia J, Corchado JC, Truhlar DG (1997) J Am Chem Soc 119: 9891
100. Tuckerman ME, Laasonen K, Sprik M, Parrinello M (1995) J Phys Chem 99: 5749
101. Tuckerman ME, Laasonen K, Sprik M, Parrinello M (1995) J Chem Phys 103: 150
102. Tunon I, Martins-Costa MTC, Millot C, Ruiz-Lopez MF (1997) J Chem Phys 106: 3633
103. Kar T, Scheiner S (1995) J Am Chem Soc 117: 1344
104. Kar T, Scheiner S (1995) Int J Quantum Chem Symp 29: 567
105. Truhlar DG, Liu YP, Schenter GK, Garrett BC (1994) J Phys Chem 98: 8396
106. Hwang JK, Warshel A (1993) J Phys Chem 97: 10053
107. Hwang JK, Warshel A (1996) J Am Chem Soc 118: 11745
108. Mauri J, Berendsen HJC (1995) J Phys Chem 99: 12711
109. Lobaugh J, Voth GA (1994) J Chem Phys 100: 3039
110. Lobaugh J, Voth GA (1996) J Chem Phys 104: 2056
111. Cao J, Voth GA (1994) J Chem Phys 100: 5106
112. Cao J, Voth GA (1994) J Chem Phys 101: 6157
113. Hammes-Schiffer S, Tully JC (1994) J Chem Phys 101: 4657
114. Hammes-Schiffer S, Tully JC (1995) J Phys Chem 99: 5793
115. Hammes-Schiffer S (1996) J Chem Phys 105: 2236
116. Drukker K, Hammes-Schiffer S (1997) J Chem Phys 107: 363
117. Morelli J, Hammes-Schiffer S (1997) Chem Phys Lett 269: 161
118. Marx D, Parrinello M (1996) J Chem Phys 102: 4077
119. Tuckerman ME, Marx D, Klein ML, Parrinello M (1997) Science 275: 817
120. Staib A, Borgis D, Hynes JT (1995) J Chem Phys 102: 2487
121. Borgis D, Hynes JT (1996) J Phys Chem 100: 1118
122. Cukier RI, Zhu J (1997) J Phys Chem 101: 7180
123. Bala P, Grochowski P, Lesyng B, Mc Cammon JA (1996) J Phys Chem 100: 2535
124. Douhal A, Lahmani F, Zewail AH (1996) Chem Phys 207: 477
125. Syage JA (1995) J Phys Chem 99: 5772
126. Kim SK, Breen JJ, Wilberg DM, Peng LW, Heikal A, Syage JA, Zewail AH (1995) J Phys Chem 99: 7421
127. Syage JA (1994) In: Manz J, Woste L (eds) Femtosecond chemistry, vol 2. VCH, Weinheim, p 475
128. Yi M, Scheiner S (1996) Chem Phys Lett 262: 567
129. Sodupe M, Oliva A, Bertran J (1997) J Phys Chem 101: 9142
130. Kohler B, Krause JL, Raksi F, Wilson KR, Yakovlev VV, Whitnell RM, Yan Y (1995) Acc Chem Res 28: 133